The effects of series resistance on the forward bias I-V characteristics in Au/Bi$_4$Ti$_3$O$_{12}$/SnO$_2$ (MFM) structures

A. TATAROĞLU, Ş. ALTINDAL, U. AYDEMİR, H. USLU
Physics Department, Faculty of Arts and Sciences, Gazi University, 06500, Ankara, Turkey

The aim of this work is to experimentally investigate the effect of series resistance (R$_s$) on current-voltage (I-V) characteristics in Au/Bi$_4$Ti$_3$O$_{12}$/SnO$_2$ (MFM) structures. The parameter R$_s$, the ideality factor (n) and barrier height ($_B$) are determined by performing different plots from the experimental forward bias I-V measurements. The current-voltage characteristics of MFM structures were measured at room temperature. The values of n and $_B$ were found to be 1.458 and 1.186 eV, respectively. The structure shows non-ideal I-V behaviour with ideality factor greater than unity. This behavior arises from the series resistance and the presence of an interfacial layer formed during the surface preparation. In addition, the values of R$_s$ were determined using Cheung's method. The effect of the series resistance for the device was not ignored and the obtained values are lower than the equivalent values obtained previously without considering effect of the presence of interfacial layer. The I-V characteristics confirmed that the distribution of R$_s$ and interfacial layer are important parameters that influence the electrical characteristics of structures.

1. Introduction

Bismuth titanate Bi$_4$Ti$_3$O$_{12}$ (BTO) thin film with a typical ferroelectric behaviour has emerged as a promising material in recent years because of its potential technological importance [1-12]. It has been extensively studied for their applications in non-volatile memories, such as ferroelectric random access memories (FeRAMs) [1-3]. Bi$_4$Ti$_3$O$_{12}$ thin film is widely preferred in device applications, since it has relatively high dielectric constant, high curie temperature, high breakdown strength, high speed read/write characteristics, large permanent polarization, low coercive field and good electro optical switching behaviour [3-5]. Furthermore, the amorphous bismuth titanite (Bi$_4$Ti$_3$O$_{12}$) films are the simplest and well known compound among the ferroelectric compounds of complex oxides [13,14].

In order to understand the characteristics of the ferroelectric random access memories (FeRAMs), Au/Bi$_4$Ti$_3$O$_{12}$/SnO$_2$ (metal-ferroelectric -metal) structures (or MFM type capacitors) have been widely studied [3,5,8,13,14]. The primary goal of this effort is to clarify some problems connected with the transport mechanism [6,8-10], as a result of surface charge (Q$_{sc}$) and the interface state density (N$_{ss}$) [2,8-11]. It is well known that ignoring the density of surface states and series resistance of the sample can lead to significant errors in the devices characteristics [15-17]. In general, there are several possible sources of error, which cause deviations of the ideal behaviour such as electrical properties. Therefore, these errors must be taken into account. These include the effects of interfacial layer; interface state (N$_{ss}$), series resistance (R$_s$) and formation of barrier height. The series resistance is an important parameter, which causes the electrical charac-teristics of devices to be non-ideal [18-22].

In this work, we report on extraction of series resistance of Au/Bi$_4$Ti$_3$O$_{12}$/SnO$_2$ (MFM) structures using the current-voltage (I-V) characteristics. The calculation of the electrical characteristics parameters such as ideality factor, barrier height and series resistance of MFM structures obtained from the experimental forward bias current-voltage (I-V) characteristics at room temperature.

2. Experimental procedure

The Bi$_4$Ti$_3$O$_{12}$ (BTO) thin films with a thickness of about 2.4 μm were deposited on tin oxide coated glass substrates by using dc-magnetron sputtering. The substrates were kept at around 700 °C. The Bi$_4$Ti$_3$O$_{12}$ target plate was prepared for sputtering by a hot compacting of Bi$_4$Ti$_3$O$_{12}$ powder of a stoichiometric composition. The mixture of Ar and O$_2$ was used as a working medium. A vacuum condensate composition is mainly determined by the condition of the formation of the layer, changed its composition, on the surface of the target depleted in component with large sputtering coefficient. In case of diffusion fluxes in a target substance at the given temperature, this process leads to the establishment of quasi-equilibrium state when the ratio of the component concentration in a surface layer of the target is inversely proportional to the corresponding sputtering components that provide the entering of the components to the working medium in a stoichiometric ratio. The chemical composition and the stoichiometry of the films were determined by local X-ray spectra method on scanning electron microscope REM-101 M by comparison of

spectral line intensity relations for the films and standard sample.

For the electrical measurements, the gold(Au) top rectifier contacts in circular shape, with a diameter of 2.5 mm and the thickness of about 2000 Å were deposited onto the films to form metal-ferroelectric-metal (MFM) structures using a shadow-mask by rf sputtering. Then the films were heated at 400 °C for 20 s by a rapid thermal annealing process to improve adhesion between metal and ferroelectrics (BTO) films. The Au/BTO/SnO₂ (MFM) structures or devices were mounted on a copper holder in a box and the electrode connections to the gold contacts for the electrical measurements were made by the use of tiny silver coated wires with silver paste. After that, the current-voltage (I-V) behaviors of MFM structures were measured by using a Keithley 614 electrometer and 220 programmable constant current sources at room temperature. All measurements were carried out with the help of a microcomputer through an IEEE-488 ac/dc converter card at room temperature.

3. Results and discussion

When a diode with an interfacial layer and series resistance R_s is considered, the current through a diode at a forward bias ($V \geq 3kT/q$), according to the thermionic emission (TE) theory, is given by [15,23,24]

$$I = AA^*T^2 \exp\left(-\frac{q\Phi_B}{kT}\right)\exp\left(\frac{q(V-IR_s)}{nkT}\right) \quad (1)$$

where V is the applied voltage across to rectifier contact, n is the ideality factor, R_s is the series resistance including bulk and contact resistance, T is the absolute temperature in K, q is the electronic charge, k is the Boltzmann constant; and I_o is the reverse saturation current and can be written as

$$I_o = AA^*T^2\exp\left(-\frac{q\Phi_B}{kT}\right) \quad (2)$$

where A is the area of rectifier contact, A* is the effective Richardson constant and Φ_B is the zero-bias barrier height. The apparent barrier height Φ_B is given by,

$$\Phi_B = \frac{kT}{q}\ln\left(\frac{AA^*T^2}{I_o}\right) \quad (3)$$

The ideality factor is a measure of the conformity of the diode to be pure thermionic emission, and it is determined from the slope of the linear region of the forward bias ln(I)-V characteristics through the relation,

$$n = \frac{q}{kT}\frac{d(V-IR_s)}{d(\ln I)} \quad (4a)$$

where d(V-IRs)/dlnI is the slope of linear region of ln(I)-V plots. Also the voltage dependent ideality factor n(V) can be written from Eq.(1) as

$$n(V) = \frac{q}{kT}\frac{(V-IR_s)}{\ln(I/I_o)} \quad (4b)$$

Fig. 1 shows the forward and reverse bias ln(I)-V characteristics of the MFM capacitor at room temperature. The current curve in forward bias quickly becomes dominated by series resistance from contact wires or bulk resistance of the semiconductor, giving rise to the curvature at high current in the semilogarithmic ln(I)-V plot. Using Eq. (2) and (4a), the values of the barrier height and the ideality factor were found to be Φ_B=1.186 eV and n=1.458, respectively.

For Schottky diode and capacitor this value of ideality factor obtained from the forward bias I-V plot are greater than unity, indicating the presence of a thin interface insulator layer between the Al layer and p-Si semiconductor. Also, such behaviour of ideality factor has been attributed to particular distribution of the interface states, the image-force effect, recombination-generation; and tunnelling may be other possible mechanisms that could lead to an ideality factor value greater than unity [17,22-27].
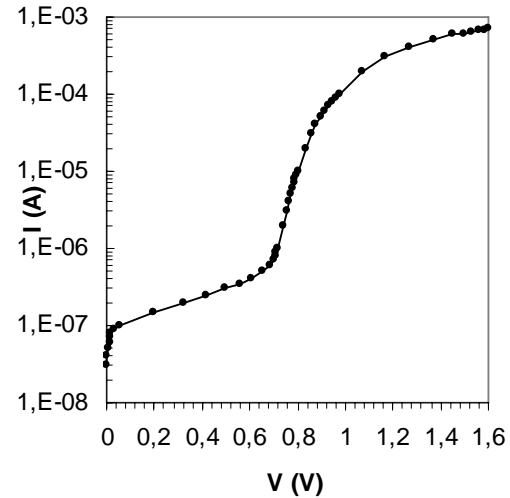

Fig. 1. The forward-bias I-V characteristics of the MFM structure at room temperature.

It should be noted that the effect of the series resistance in the linear region of forward bias I-V plot could be neglected in Fig. 1, but deviate considerably from the linearity due to the effect of series resistance, the interfacial layer, and the interface states when the applied voltage is sufficiently large. In addition, the current rises slowly with the applied reverse bias and does not show any effect of saturation. This soft or slight non-saturating behaviour of reverse current may be explained in terms of the image force lowering of Schottky barrier height [23] and the presence of the interfacial layer [17,23].

Usually, the forward bias current voltage (I-V) characteristics are linear in the semilogarithmic scale at low voltages but deviate considerably from linearity due to the effect of parameters such as the R_s and the N_{ss} when the applied voltage is sufficiently large. The values of series resistance R_s were carried out using another method developed by Cheung [28]. The Cheung's functions given as,

$$\frac{dV}{d(\ln I)} = IR_s + n\left(\frac{kT}{q}\right) \tag{5}$$

$$H(I) = V - n\left(\frac{kT}{q}\right)\ln\left(\frac{I}{AA^*T^2}\right) \tag{6}$$

and H(I) is given as follows:

$$H(I) = IR_s + n\Phi_B \tag{7}$$

should give a straight line for the data of downward curvature region in the forward bias I-V characteristics. The term IR_s is the voltage drop across the series resistance of capacitor. In Fig. 2(a) and (b), the experimental $dV/d\ln I$ vs I, and H(I) vs I plots are for the MFM structure, respectively. Thus, the values of R_s and nkT/q have been obtained from the slope and y-axis intercepts of the plot dV/dlnI vs I.

Table 1. Various parameters determined from I-V characteristics of MFM structure.

I_o (A)	n	Φ_B (eV)	R_s(dV/d(lnI)) (Ω)	R_s(H(I)) (Ω)	W_D (cm)	N_{ss} (eV^{-1}cm^{-2})
6.13×10^{-15}	1.458	1.186	383.77	371.85	5.45×10^{-4}	3.02×10^{11}

Also, Fig. 2(b) obtained from Eq. (11) shows the plot of H(I) vs I and gives a straight line with the y-axis intercept equal to $n\Phi_B$. The slope of this plot also provides the second determination of R_s, which can be used to check the consistency of Cheung's approach. The values of series resistance calculated from Eqs. (5) and (7) are

presented in Table 1. As can be seen in Table 1, the values of series resistance R_s(dV/dlnI) and R_s(H(I)) calculated from Cheung's functions dV/dlnI and H(I) respectively are in good agreement with each other [29-32].
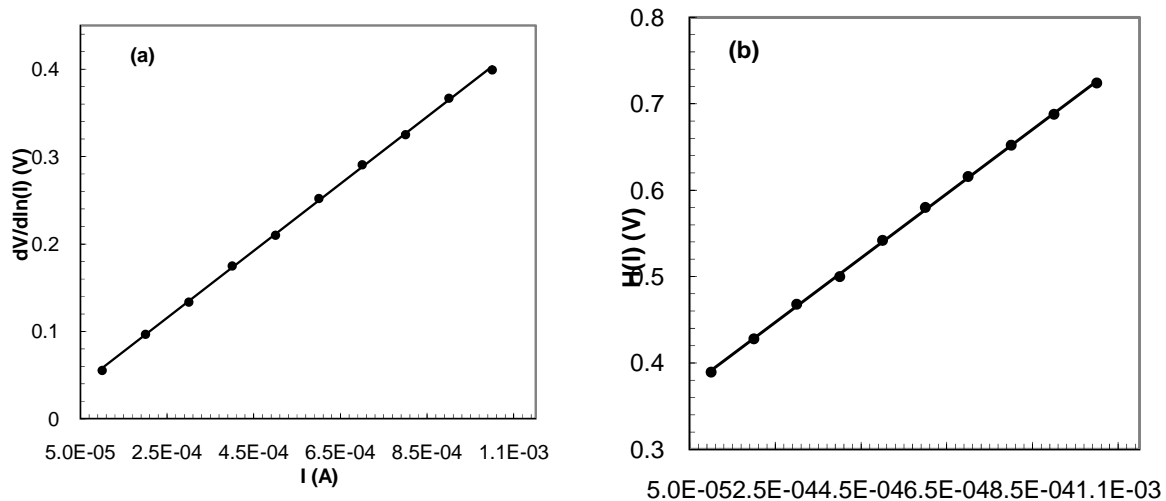

Fig. 2. (a) Experimental dV/dlnI vs plots for the MFM structure; (b) Experimental H(I) vs I plots for the MFM structure.

4. Conclusions

In this study, the electrical properties of $Au/Bi_4Ti_3O_{12}/SnO_2$ (MFM) structures have been characterized by using the current-voltage (I-V) characteristics at room temperature. The non-ideal forward bias I-V behavior observed in the structure is attributed to a change in the metal /semiconductor barrier height due to

the interface states, the interfacial layer and series resistance. The applied bias voltage drops partially across the interfacial layer causing the forward current to drop, thus this case has resulted in strong deviation from the ideal I-V characteristics. The values of ideality factor and barrier height have been calculated as 1.458 and 1.186 eV, respectively, from forward bias I-V measurements. The n values obtained from I-V characteristics are higher than

unity, and that is attributed to the presence of an interfacial layer. The downward curvature at sufficiently large voltages is caused by the effect of series resistance R$_s$, apart from the presence of the interface states, which are in equilibrium with the semiconductor. The value of the R$_s$ has been calculated from high voltage region of the structure by using Cheung functions. It is seen that there is a good agreement between the values of the series resistance obtained from two Cheung plots.

It is clear that ignoring the role of series resistance, interface state density and interfacial layer can lead to significant errors in the electrical characteristics of devices.

References

[1] B. H. Park, S. J. Hyun, J. Appl. Phys. **84**, 4428 (1998).
[2] F. Scott, C. A. Arauzo, Science **246**, 1400 (1989).
[3] L. B. Kong, J. Ma, Thin Solid Films **379**, 89 (2000).
[4] Z. H. Bao, Y. Y. Yao, J. S. Zhu, Y. N. Wang, Materials Letters **56**, 861 (2002).
[5] P. C. Joshia, S. B. Krupandin, J. Appl. Phys. **72**, 5517 (1992).
[6] H. J. Cho, W. Jo, T. W. Noh, Appl. Phys. Lett. **65**, 1525 (1994).
[7] C. Fangago, G. A. Saunders, E. F. Lambson, R. N. Hampton, G. Garini, G. D Marco, M. Lanza, J. Polymer Sci: Part B: Polymer Phys. **34**, 425 (1996).
[8] L. Wei, M.A. Jun, S. Chun-Hua, B. Peng, L. Xiao-Mei, Z. Jin-Song, W. Ye-Ning, Chin. Phys. Lett. **21**, 544 (2004).
[9] W. Jo, K.H. Kim, T. W. Noh, Appl. Phys. Lett. **66**, 3120 (1995).
[10] W. L. Waren, G. E. Pike, B. A. Tuttle, D. Dimos, Appl. Phys. Lett. **70**, 2010 (1997).
[11] A. Q. Jiang, G. H. Li, L. D. Zhang, J. Appl. Phys. **83**, 4878 (1998).
[12] X. J. Zhang, S. T. Zhang, Y. F. Chen, Z. G. Liu, N. B. Ming, Microelect. Eng. **66**, 719 (2003).
[13] J. Y. Gu, C. Kwon, M. C. Robson, Z. Trajanovic et al., Appl. Phys. Lett. **70**, 1763 (1997).
[14] F. M. Pontes, E. R. Leite, E. J. H. Lee, E. Longo, J. A. Varela, Thin Solid Films **385**, 260 (2001).
[15] S. M. Sze, Physics of Semiconductors Devices, John Wiley & Sons, New York, 1981.
[16] E. H. Nicollian, J. R. Brews, MOS (Metal-Oxide-Semiconductor) Physics and Technology, John Wiley& Sons, New York, 1982.
[17] H. C. Card, E. H. Rhoderick, J. Phys. D **4**, 1589 (1971).
[18] M. O. Aboelfotoh, J. Appl. Phys. **69**(5), 3351 (1991).
[19] R. Castagne, A. Vapaille, Surface Science **28**(1), 157 (1971).
[20] H. Deuling, E. Klausmann, A. Goetzberger, Solid State Electron. **15**(5), 559 (1972).
[21] M. K. Hudait, S. B. Krupanidhi, Solid State Elect. **44**, 1089 (2000).
[22] E. H. Nicollian, A. Goetzberger, Appl. Phys. Lett. **7**, 216 (1965).
[23] E. H. Rhoderick, R. H. Williams, Metal-Semiconductor Contacts, 2nd Ed., Clarendon Press, Oxford, 1988.
[24] S. Ashok, J. M. Borrego, R. J. Gutmann, Solid-State Electron. **22**, 621 (1979).
[25] P. Chattopadhyay, A. N. Daw, Solid State Electron. **29**(5), 555 (1986).
[26] F. Parlaktürk, Ş. Altındal, A. Tataroğlu, M. Parlak, A. Agasiev, Microelectron. Eng., **85**, 81 (2008).
[27] A. Tataroğlu, Ş. Altındal, Microelectronic Eng. **83**, 582 (2006).
[28] S. K. Cheung, N. W. Cheung, Appl. Phys. Lett. **49**(2), 85 (1986).
[29] B. Akkal, Z. Benemara, A. Boudissa, N. B.Bouiadjra, M. Amrani, L. Bideux, B. Gruzza, Mater. Sci. And Eng.B **55**, 162 (1998).
[30] S. Kar, K. M. Panchal, S. Bhattacharya, S. Varma, IEEE Trans. Electron Dev. **29**, 1839 (1982).
[31] M. Y. Feteha, M. Soliman, N. G. Gomaa, M. Ashry, Renew. Energy **26**, 113 (2002).
[32] L. Beji, T. Ben Jomaa, Z. Harrabi, A. Laribi, A. Missaoui, A. Bouazizi, Vacuum **80**, 480 (2006).

*Corresponding author: uaydemir@gazi.edu.tr